



저작자표시-비영리-동일조건변경허락 2.0 대한민국

이용자는 아래의 조건을 따르는 경우에 한하여 자유롭게

- 이 저작물을 복제, 배포, 전송, 전시, 공연 및 방송할 수 있습니다.
- 이차적 저작물을 작성할 수 있습니다.

다음과 같은 조건을 따라야 합니다:



저작자표시. 귀하는 원저작자를 표시하여야 합니다.



비영리. 귀하는 이 저작물을 영리 목적으로 이용할 수 없습니다.



동일조건변경허락. 귀하가 이 저작물을 개작, 변형 또는 가공했을 경우에는, 이 저작물과 동일한 이용허락조건하에서만 배포할 수 있습니다.

- 귀하는, 이 저작물의 재이용이나 배포의 경우, 이 저작물에 적용된 이용허락조건을 명확하게 나타내어야 합니다.
- 저작권자로부터 별도의 허가를 받으면 이러한 조건들은 적용되지 않습니다.

저작권법에 따른 이용자의 권리는 위의 내용에 의하여 영향을 받지 않습니다.

이것은 [이용허락규약\(Legal Code\)](#)을 이해하기 쉽게 요약한 것입니다.

[Disclaimer](#)

공학석사학위논문

압전 에너지 하베스팅 스킨의 가용 전력
최대화 연구

Power Usage Maximization of a Piezoelectric Energy
Harvesting Skin

2014 년 2 월

서울대학교 대학원

기계항공공학부

조 철 민

압전 에너지 하베스팅 스킨의 가용 전력 최대화 연구

Power Usage Maximization of a Piezoelectric Energy
Harvesting Skin

지도교수 윤 병 동

이 논문을 공학석사 학위논문으로 제출함

2014 년 2 월

서울대학교 대학원

기계항공공학부

조 철 민

조철민의 공학석사 학위논문을 인준함

2013 년 12 월

위 원 장 _____ 김 윤 영 _____ (인)

부위원장 _____ 윤 병 동 _____ (인)

위 원 _____ 김 도 년 _____ (인)

Abstract

Power Usage Maximization of a Piezoelectric Energy Harvesting Skin

Chulmin Cho

School of Mechanical and Aerospace Engineering

The Graduate School

Seoul National University

Recently, piezoelectric energy harvesting (PEH) technology that harvests electrical energy from ambient vibration energy has emerged as a solution to eliminate the need for batteries in wireless sensors. Previous studies on PEH devices have focused on a cantilever type because this type can use a resonance effect for large strain to harvest a large amount of electric energy. Although cantilevered PEH devices have merits, their practical applications are limited by at least three disadvantages. First, cantilever-type PEH devices require an additional space due to a tip mass and a clamping structure. Second, cantilever-type PEH devices are vulnerable to external shock and dust. Finally, the clamping part of the PEH device can loosen after the exposure to long-term vibration. In order to overcome drawbacks, a PEH skin, which generates electrical energy by directly attaching a thin piezoelectric layer onto a vibrating skin structure as one embodiment was proposed as an alternative type. Previous works of the PEH skin are focused on designing strain inflection lines to minimize the voltage cancellation effect.

This research proposes a new way of optimizing the impedance matching design

variable of the PEH skin to maximize power usage for the target electrical load. The proposed design process involves three steps. First, the output power of the PEH skin is analytically expressed in terms of measurable variables. Second, the limiting behavior of the PEH skin is studied to find the characteristics of the PEH skin. Finally, the optimal size of the PEH skin is derived to maximize power consumption for the specific electrical load. The validity of the proposed design method is demonstrated through experimental analysis. The results show a good agreement.

Keywords: Piezoelectric
Energy harvesting
Piezoelectric energy harvesting (PEH) skin
Impedance matching

Student Number: 2012-20707

Table of Contents

Abstract	i
List of Tables.....	v
List of Figures	vi
Nomenclature	vii
Chapter 1. Introduction.....	1
1.1 Motivation.....	1
1.2 Organization of Thesis.....	4
Chapter 2. Background and Literature Review.....	6
2.1 Background of Piezoelectric Energy Harvesting	6
2.1.1 Piezoelectric Effect.....	6
2.1.2 Piezoelectric Materials.....	8
2.1.3 Impedance Matching	9
2.2 Literature Review: Prior Piezoelectric Energy Harvesting (PEH)	
Research	11

Chapter 3. Proposed Analytical Approach to Maximize Power of a PEH Skin.....	17
3.1 Mathematical Modeling of PEH Skin	17
3.2 Analytical Analysis of PEH Skin	20
3.2.1 Asymptotic Analysis of PEH Skin	21
3.2.2 Impedance Matching for Power Maximization.....	22
 Chapter 4. Experimental Validation	25
4.1 Experimental Setup.....	25
4.2 Experimental Results.....	27
4.2.1 Validation of Limiting Behavior	27
4.2.2 Validation of Optimized PEH Skin Size.....	29
 Chapter 5. Conclusion	33
5.1 Contributions.....	33
5.2 Future Work.....	34
 Bibliography.....	36
국문 초록	40

List of Tables

Table 1 Material properties of PZT (PSI-5H4E, Piezo Systems, Inc.).....	9
Table 2 Summary of optimum load derived from both the mathematical model and the experiments (Unit: Ω)	31
Table 3 Backward estimation of the PEH skin size	32

List of Figures

Figure 1-1 Figure of a cantilever-type piezoelectric energy harvesting device	2
Figure 2-2 Source and Load parts of an electric circuit.....	10
Figure 2-3 Maximum power transfer theorem.....	11
Figure 2-4 A schematic representation of cantilever-type piezoelectric energy harvesting devices, (a) unimorph and (b) bimorph.....	12
Figure 2-6 A schematic representation of the voltage cancelation effect.....	15
Figure 2-7 Prevention of the voltage cancelation effect by material segmentation	15
Figure 3-1 A schematic representation of PEH skin.....	17
Figure 4-1 Experimental setup.....	26
Figure 4-2 Close view of the PEH skin with a clamping device	26
Figure 4-3 Limiting behavior validation for harvested (a) voltage, (b) current, and (c) power.....	28
Figure 4-4 Comparison of the output power at (a) 48.65 Hz, (b) 69.5 Hz, and (c) 90.35 Hz	30

Nomenclature

T	mechanical stress
S	mechanical strain
D	electric displacement
E	electric field
c_j^E	elastic modulus of the piezoelectric layer at constant electric field
s_{ij}^E	compliance of the piezoelectric layer at constant electric field
ϵ_0	absolute permittivity
$\bar{\epsilon}_{ij}^S$	relative permittivity at constant strain
$\bar{\epsilon}_{ij}^T$	relative permittivity at constant stress
\bar{e}	piezoelectric constant
h_p	thickness of the piezoelectric layer
A	area of the PEH (Piezoelectric energy harvesting) skin
R_L	external resistance
ω	target system frequency
$v(t)$	output voltage response
V	output voltage amplitude
I	output current amplitude
P	output power amplitude

Chapter 1. Introduction

1.1 Motivation

Recent developments in sensing technology have enabled a new generation of technological applications. The dream of the future is that ubiquitous networks of smart wireless sensing nodes will enrich our daily lives as well as advance industrial technology, such as structural health monitoring (SHM) and the Internet of Things (IoT). To realize these future possibilities, countless wireless sensors will need to be built into wireless sensor networks (WSN). However, in order to provide sensing networks that are truly autonomous, we must develop methods to eliminate the need for batteries (which require human interaction for charging or changing) in these wireless sensors. The limited life expectancy and high replacement cost of batteries limit current applications of wireless sensor nodes. If the need for batteries can be eliminated, wireless sensors are likely to become widespread in many areas of life.

Piezoelectric energy harvesting (PEH) technology, a technique that harvests electrical energy from ambient energy sources, has emerged as a possible solution to eliminate the need for batteries in wireless sensor nodes (Sodano, Inman et al. 2004, Beeby, Tudor et al. 2006). Among various external energy sources (e.g. solar power, thermal energy, wind energy, salinity gradients, kinetic energy, and biological energy), vibration energy has received attention due to its high energy density and its energy conversion efficiency (Cook-Chennault, Thambi et al. 2008).

Previous studies on PEH devices have focused on a cantilever type of PEH device because this type can use a resonance effect for large strain to harvest a large amount of electric energy. Although cantilevered PEH devices have merits, their practical applications are limited by at least three disadvantages. First, cantilever-type PEH devices require a large physical space due to their tip mass and the need for an additional clamping structure, as shown in Figure 1-1. Second, cantilever-type PEH devices are vulnerable to external shock and dust. Thus, this type of PEH device needs to be implemented in conjunction with a protective structure to enable a longer life span. Finally, the clamping part of the PEH device can loosen after long-term vibration. Loosening of the clamping leads to a dramatic loss of harvested power.

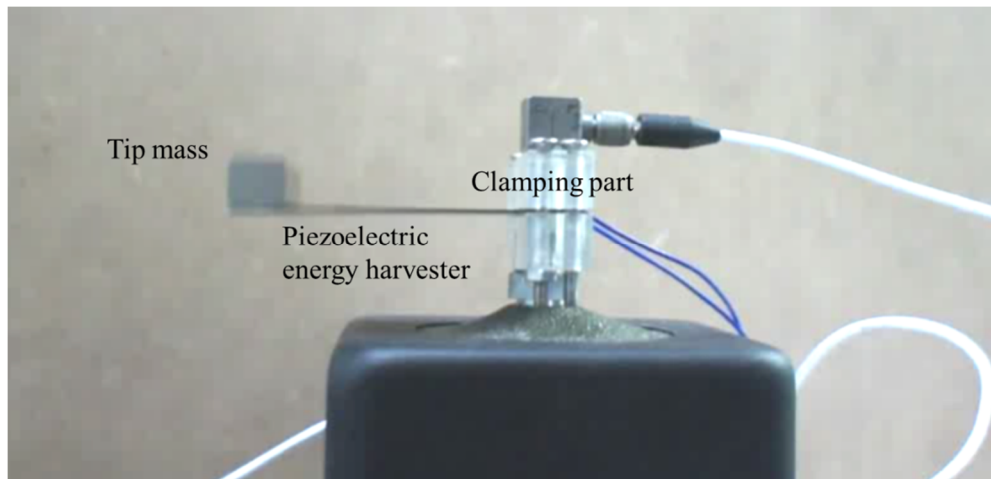


Figure 1-1 Figure of a cantilever-type piezoelectric energy harvesting device

To solve the aforementioned drawbacks found in cantilever-type PEH devices, a skin-type PEH device, called a “PEH skin” (Lee and Youn 2011) was proposed. Unlike the cantilever-type PEH devices that take advantage of resonance, the PEH skin cannot use resonance because systems targeted for PEH applications (such as outdoor air-conditioning units) are designed to avoid resonance. Instead, the strain inflection line has been employed to reduce the voltage cancelation effect that happens in a piezoelectric material (Lee, Youn et al. 2009). The reduction of the voltage cancelation effect can be carried out successfully by removing the piezoelectric material on the strain inflection line where the amount of in-plane strain is inconsiderable (Erturk, Tarazaga et al. 2009). It is important to note that attaching piezoelectric materials to the whole substrate area inside the inflection line is undesirable because it results in high-cost (added expensive material) and low-efficiency of the PEH skin.

Meanwhile, impedance matching is an electrical engineering technique used to maximize power transfer from PEH devices to the external load (Kim, Priya et al. 2007, Kong, Ha et al. 2010). These electrical engineering efforts are limited, however, because researchers consider the mechanical portions of the PEH devices to be a given condition and thus only concentrate on optimizing the electric circuit of PEH devices.

This work presents a new way of optimizing the impedance-matching design variable of a PEH skin to maximize power usage for specific electrical resistance. The proposed design process involves three steps. First, the output power of the PEH skin is analytically expressed in terms of measurable variables, such as piezoelectric

material size, strain on piezoelectric material, target system frequency, and external resistive load (which is regarded as the target application in the thesis). Second, derived solutions with measurable variables are used to reveal the characteristics of the PEH skin. Asymptotic analysis is used to reveal the limiting behavior of the PEH skin. The optimal resistive load that generates the maximum output power is also found. Finally, in the third step, the relationship between the optimal size of the PEH skin and the maximum output power is determined. As the value of external resistive load is given in the third step, the maximum output power can be considered as maximum power usage for specific electrical resistive load. The validity of the design proposed using this new method is demonstrated by comparing with experimental results.

1.2 Organization of Thesis

This thesis consists of five chapters. Chapter 2 gives background information about PEH and reviews previous PEH research. It helps readers to understand the overall contents of the thesis. Chapter 3 presents the proposed analytical approach to power maximization of the PEH skin. In this chapter, a new process of using analytical solutions is used to derive the size of the PEH skin that will maximize power usage for specific electrical load. Chapter 4 shows the experimental validation of the method proposed in this work. In this chapter, the limiting behavior of the PEH skin and the PEH skin size that generates the maximum power usage that were derived from our new method (chapter 3) are validated by comparison with

experimental results. Chapter 5 summarizes the study and the contributions of the research. Also, this chapter discusses future work that will complement the work outlined in the thesis.

Chapter 2. Background and Literature Review

PEH studies include aspects of mechanical engineering, material science, and electrical engineering. As such, a multi-disciplinary approach is adopted here to helpfully explain PEH technology.

Section 2.1 presents background information on the basics of PEH. First, the piezoelectric effect, which is the basis for piezoelectric energy harvesting, is explained. Next, piezoelectric material properties that determine performance of PEH are introduced. Finally, general knowledge about impedance matching – which is the core concept in this thesis – is provided. Section 2.2 reviews previous PEH research. Processes for mathematical modeling are discussed, as is the structure type of PEH devices. Finally, this section examines efforts to raise energy conversion efficiency through electrical engineering.

2.1 Background of Piezoelectric Energy Harvesting

2.1.1 Piezoelectric Effect

In 1880, physicists Jacques and Pierre Curie demonstrated the special electric charge called piezoelectricity for the first time. Piezoelectricity is created in certain materials in response to applied mechanical force (Manbachi and Cobbold 2011).

Later, they explained this experiment as the direct piezoelectric effect (Curie and Curie 1880). The direct piezoelectric effect is the internal generation of electrical charge resulting from an applied mechanical stress.

However, there is not only a direct piezoelectric effect but also an inverse piezoelectric effect in piezoelectric material at the same time. The inverse piezoelectric effect is the internal generation of a mechanical strain resulting from an applied electric field.

These two effects coexist in certain crystalline material, as shown in Figure 2-1. The piezoelectric effect can be explained as the linear electromechanical interaction between the mechanical and the electrical region in a piezoelectric material (Gautschi 2002). PEH uses the direct piezoelectric effect to scavenge energy.

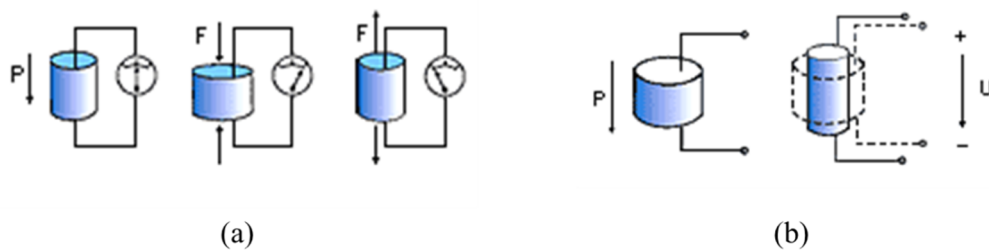


Figure 2-1 (a) direct piezoelectric effect and (b) inverse piezoelectric effect

2.1.2 Piezoelectric Materials

There are many natural crystalline materials that exhibit piezoelectric behavior, including bone, sucrose, quartz, Rochelle salt, silk, and DNA (Skoog, Holler et al. 1998). However, these materials are not ideal for PEH because of their low-energy density. Among the many piezoelectric materials, two offer the highest-energy density, making them ideal candidates for PEH. These high-energy-density materials are PVDF and PZT.

PVDF (polyvinylidene difluoride) is a piezoelectric polymer which has been used in many applications including microphones, sensors and actuators (Vinogradov, Hugo Schmidt et al. 2004). Because PVDF is a kind of polymer group, it has a flexible and bendable nature.

PZT (lead zirconate titanate) is one of the most suitable synthetic ceramics for piezoelectric energy harvesting due to its high piezoelectric and dielectric constant. These material properties of PZT are greater than those of PVDF (Higashihata, Yagi et al. 1986). However, the use of PZT in piezoelectric energy harvesting devices is limited because it is brittle and fragile.

Between these two materials, PZT is the more desirable material for piezoelectric energy generation due to its higher energy density, as compared to PVDF. When using PZT material in PEH devices, it is important to design the device carefully to combat the brittle and fragile characteristics of PZT.

In this work, commercial PZT (PSI-5H4E, Piezo Systems, Inc.) is used for demonstration. The material properties of the selected PZT are summarized in Table1.

Table 1 Material properties of PZT (PSI-5H4E, Piezo Systems, Inc.)

density (kg/m ³)	7800	s_{11}^E (m ² /N)	1.61×10^{-11}
d_{15} (m/V)	7.41×10^{-10}	s_{12}^E (m ² /N)	-4.84×10^{-12}
d_{31} (m/V)	-3.20×10^{-10}	s_{13}^E (m ² /N)	-6.00×10^{-12}
d_{33} (m/V)	6.50×10^{-10}	s_{33}^E (m ² /N)	2.00×10^{-11}
ϵ_{11}^T (relative)	3800	s_{44}^E (m ² /N)	5.20×10^{-11}
ϵ_{33}^T (relative)	3800	s_{66}^E (m ² /N)	4.19×10^{-11}

2.1.3 Impedance Matching

One of the most important themes in building a piezoelectric energy harvesting circuit is impedance matching. Impedance matching is defined as the practice of designing the input impedance of a resistive electrical load to maximize the power transfer.

Generally, a circuit can be divided into two parts: the source and the load (see Figure 2-2). The maximum power transfer theorem says that to transfer the maximum amount of power from a source to a load, the load impedance should match the source impedance. In a basic circuit like Figure 2-2, maximum power is transferred from a

source to a load when the load impedance equals the internal impedance of the source. Figure 2-3 reveals that matching load and source impedances will achieve maximum power at the same impedance.

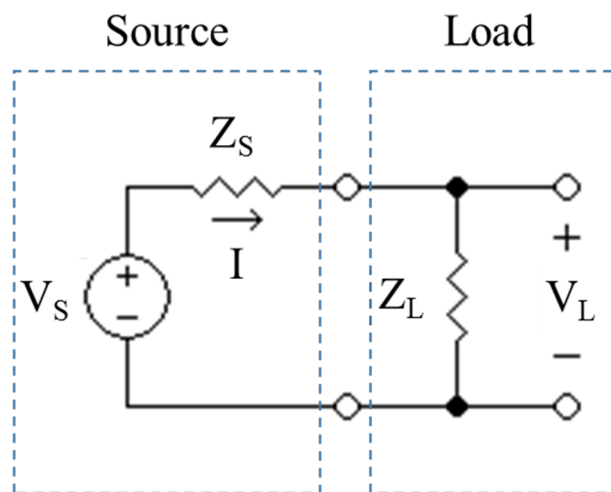


Figure 2-2 Source and Load parts of an electric circuit

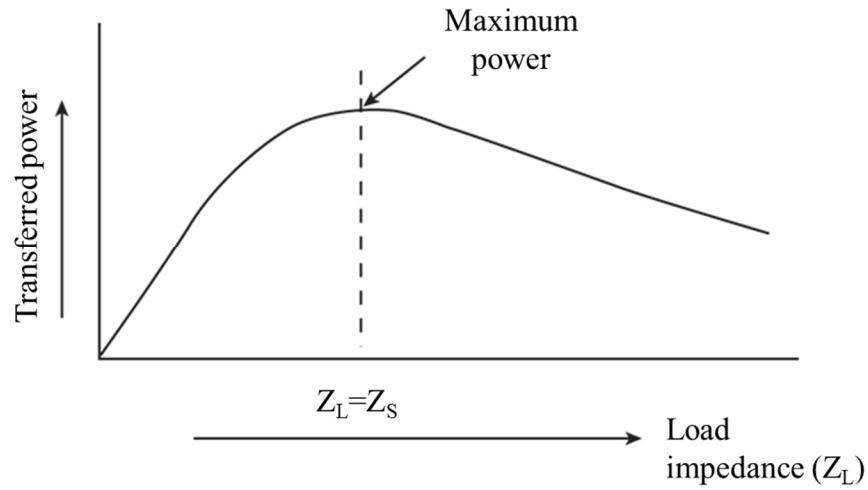


Figure 2-3 Maximum power transfer theorem

2.2 Literature Review: Prior Piezoelectric Energy Harvesting (PEH) Research

Most previous PEH work has examined cantilever-type devices. This type of device has merits for scavenging vibration energy because its natural frequency is low and its mechanical strain near clamping part is very high. A schematic representation of a cantilever-type PEH device is shown in Figure 2-4. Among PEH devices of this type, a cantilever beam with a single piezoelectric layer is called a unimorph energy harvester and one with two piezoelectric layers is called a bimorph energy harvester.

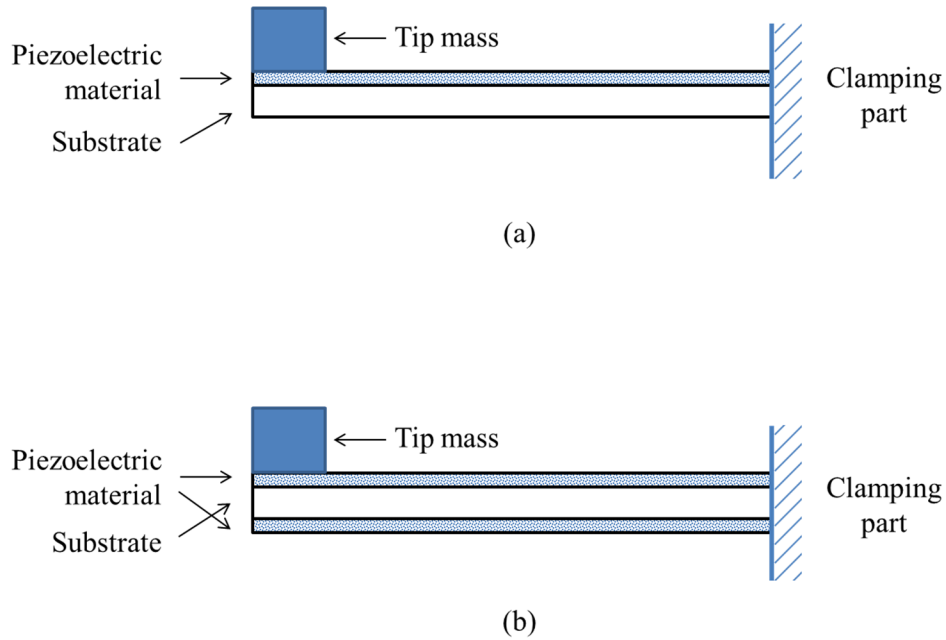


Figure 2-4 A schematic representation of cantilever-type piezoelectric energy harvesting devices, (a) unimorph and (b) bimorph

Prior work related to mathematical modeling of a cantilevered PEH device was derived from an elementary vibration text book (Rao 2003). Stephen proposed mathematical modeling of a cantilever type PEH device with lumped parameters (Stephen 2006). However, a cantilevered PEH device usually does not have a large proof mass. As a result, lumped parameter modeling – which neglects the inertial effect of the distributed mass to the excitation amplitude – is an inherently inaccurate modeling strategy (Erturk and Inman 2008).

The Rayleigh-Ritz method, which gives a spatially discretized model of the distributed parameter system, was adopted to improve accuracy of the modeling (Dutoit, Wardle et al. 2005). However, according to subsequent experiments, the Rayleigh-Ritz method was not accurate in the resonance frequency region (DuToit and Wardle 2007).

More sophisticated analytical solutions based on distributed parameter electromechanical modeling have since been developed, along with experimental validations (Erturk and Inman 2008). Although the proposed solutions are complex, as compared to previous models they show an excellent predictability based on the experimental results (Erturk and Inman 2009). This modeling has thus become the cornerstone for ongoing research related to cantilever-type piezoelectric energy harvesting devices.

In addition to the cantilevered PEH device, another PEH device type of interest is a skin-type device that is called PEH skin, as shown in Figure 2-5. The PEH skin consists of thin piezoelectric materials directly attached to a vibrating shell structure, which can be found in various kinds of mechanical systems. Contrary to the cantilever type of energy harvester, the PEH skin does not take advantage of the resonance effect. This is because of the characteristics of the system in which it is designed to be applied; these systems are designed to avoid resonance.

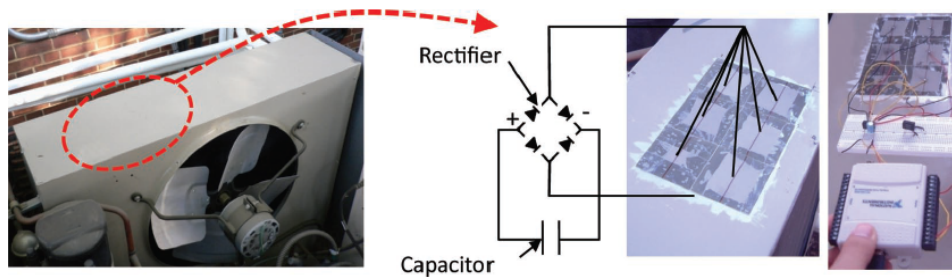


Figure 2-5 Piezoelectric energy harvesting (PEH) skin at an early stage (Lee and Youn 2011)

To improve the efficiency of piezoelectric energy harvesting devices in a mechanical way, previous researchers considered the voltage cancelation effect. The voltage cancelation effect happens when a piezoelectric material encounters compressive and tensile strains together, as shown in Figure 2-6 (Lee, Youn et al. 2009). A solution proposed to limit the voltage cancelation effect is the material segmentation method (see Figure 2-7) (Erturk, Tarazaga et al. 2009, Lee, Youn et al. 2009, Erturk 2011, Lee and Youn 2011). Removing the piezoelectric material on the strain inflection line where the amount of in-plane strain is inconsiderable reduces the voltage cancelation effect.

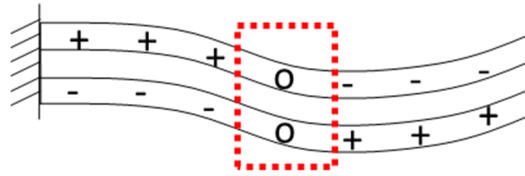


Figure 2-6 A schematic representation of the voltage cancellation effect

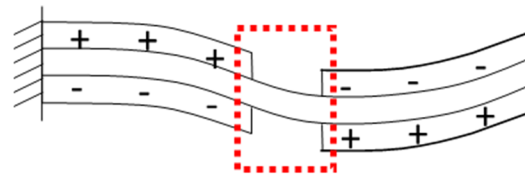


Figure 2-7 Prevention of the voltage cancellation effect by material segmentation

Meanwhile, electrical engineers have researched piezoelectric energy harvesting circuits to attempt to attain high energy conversion efficiency between the piezoelectric energy harvester and target components, such as wireless sensors.

The optimal DC voltage required to maximize the power extraction under the direct connection of the load to an AC-DC rectifier of a piezoelectric power generator has been derived (Kim, Priya et al. 2007). Badel et al. developed circuits to increase piezoelectric power generation that incorporated electronic switches and inductors to shape the delivered voltage (Badel, Guyomar et al. 2006). Na Kong et al. presented a new approach for impedance matching to maximize the power extraction (Kong,

Ha et al. 2010). In addition, energy flow was investigated to help energy conversion efficiency research (Liang and Liao 2011).

Chapter 3. Proposed Analytical Approach to Maximize Power of a PEH Skin

Section 3.1 covers the method chosen in this work for mathematical modeling of piezoelectric power generation from the PEH skin. The analytical expressions for a circular PZT patch attached to a substrate (see Figure 3-1) were derived to predict the power output based on the induced dynamic strain. The overall modeling procedure outlined in section 3.1 follows the method outlined in a prior study carried out by A.Erturk (Erturk 2011). The solutions derived in section 3.1 were employed to propose a new PEH skin design, as outlined in section 3.2.

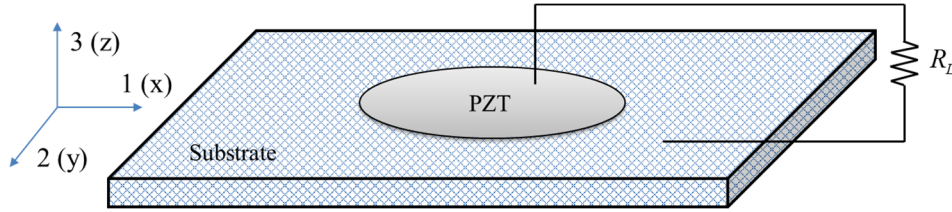


Figure 3-1 A schematic representation of PEH skin

3.1 Mathematical Modeling of PEH Skin

The piezoelectric effect is the linear electromechanical interaction between the mechanical and the electrical state in crystalline materials such as PZT. According

to IEEE Std 176 (1988), the linear constitutive equations for piezoelectric materials are given by Equation (1) and (2).

$$T_{ij} = c_{ijkl}^E S_{kl} - e_{kij} E_k \quad (1)$$

$$D_i = e_{ikl} S_{kl} + \varepsilon_{ij}^S E_k \quad (2)$$

where T is the mechanical stress, S is the mechanical strain, D is the electric displacement, and E is the electrical field.

Since the only source of mechanical strain is assumed to be the axial strain due to bending, for the given electrode configuration, the tensorial representation of the relevant piezoelectric constitutive equation that gives the vector of electric displacements can be reduced to the following scalar equation.

$$D_3 = \bar{e}_{31} (S_1 + S_2) + \bar{\varepsilon}_{33}^S E_3 \quad (3)$$

where D_3 is the electric displacement component along the z-axis and $\bar{\varepsilon}_{33}^S$ is the permittivity component at constant strain. Assuming that the electrodes of the PZT patch are connected to an external resistive load, R_L , the electric relationship can be obtained from Ohm's law and the integral form of Gauss's law as:

$$\frac{d}{dt} \left(\oint_A (\bar{e}_{31} (S_1 + S_2) + \bar{\varepsilon}_{33}^S E_3) dA \right) = \frac{v(t)}{R_L} \quad (4)$$

Equation (4) can be rewritten by expressing the uniform electric field in terms of

the electric potential difference as:

$$\frac{dv(t)}{dt} + \frac{h_p v(t)}{R_L \bar{\epsilon}_{33}^S A} = \frac{h_p \bar{e}_{31}}{\bar{\epsilon}_{33}^S A} \oint_A \frac{\partial}{\partial t} (S_1 + S_2) dA \quad (5)$$

where A is the area of the PZT and h_p is the thickness of the PZT.

To determine the steady-state power output in harmonic vibration, let the dynamic strain components be harmonic at the same frequency for simplicity:

$$S_1 = \widetilde{S}_1 e^{j\omega t}, S_2 = \widetilde{S}_2 e^{j\omega t} \quad (6)$$

where ω is the frequency, j is the unit imaginary number, and \widetilde{S}_1 and \widetilde{S}_2 are the strain values. If the steady-state voltage output is $v(t) = V e^{j\omega t}$ Equation (5) can be reduced to:

$$v(t) = \frac{j\omega \bar{e}_{31} R_L h_p A (\widetilde{S}_1 + \widetilde{S}_2)}{j\omega R_L \bar{\epsilon}_{33}^S A + h_p} e^{j\omega t} \quad (7)$$

Therefore, the steady-state voltage amplitude is:

$$V = \frac{j\omega \bar{e}_{31} R_L h_p A (\widetilde{S}_1 + \widetilde{S}_2)}{j\omega R_L \bar{\epsilon}_{33}^S A + h_p} \quad (8)$$

In addition, the steady-state current amplitude is:

$$I = \frac{j\omega\bar{e}_{31}h_pA(\widetilde{S}_1 + \widetilde{S}_2)}{j\omega R_L\bar{\varepsilon}_{33}^sA + h_p} \quad (9)$$

Finally, the steady-state power amplitude is given by:

$$P = \frac{\omega^2\bar{e}_{31}^2R_Lh_p^2A^2(\widetilde{S}_1 + \widetilde{S}_2)^2}{\omega^2R_L^2(\bar{\varepsilon}_{33}^s)^2A^2 + h_p^2} \quad (10)$$

3.2 Analytical Analysis of PEH Skin

Equations (8)~(10) show that the amount of harvested voltage, current, and power are correlated with measurable variables: PZT patch size, A , sum of strain on PZT patch, $\widetilde{S}_1 + \widetilde{S}_2$, external resistive load, R_L , and target system frequency, ω . Among these variables, external resistive load and target system frequency are considered to be known constant variables in the design process in this study. These are considered known because target system frequency can be measured for target systems of interest, such as outdoor air-conditioning units. Likewise, the external resistive load can be determined once a specific target application (such as a wireless sensor) is selected.

Therefore, the design parameters of the PEH skin are the PZT patch size and the

strain on PZT patch. It is important to note that strain on the PZT patch is dependent on PZT patch size and location. As a result, determination of the PZT patch size and location is an important part of the PEH skin design process.

3.2.1 Asymptotic Analysis of PEH Skin

First, asymptotic analysis was conducted to investigate the characteristics of the PEH skin. Limiting behaviors of the output voltage are:

$$\lim_{R_L \rightarrow 0} V = 0 \quad (11)$$

$$\lim_{R_L \rightarrow \infty} V = \frac{\bar{e}_{31} h_p}{\bar{\epsilon}_{33}^S} (\widetilde{S}_1 + \widetilde{S}_2) \quad (12)$$

Limiting behaviors of the output voltage show that there is a positive correlation between the harvested output voltage and the external resistive load. This is especially true when the circuit is in an open condition, as output voltage is proportional to the sum of strains.

In sequence, asymptotic analysis of the output current is given by:

$$\lim_{R_L \rightarrow 0} I = j\omega \bar{e}_{31} A (\widetilde{S}_1 + \widetilde{S}_2) \quad (13)$$

$$\lim_{R_L \rightarrow \infty} I = 0 \quad (14)$$

Unlike in the case of voltage, a negative correlation between current and the load is described in Equations (13) and (14). Also, generated current in a short-circuit condition is proportional to the mechanical strain of the PEH skin.

Finally, the limiting behaviors of the output power are:

$$\lim_{R_L \rightarrow 0} P = 0 \quad (15)$$

$$\lim_{R_L \rightarrow \infty} P = 0 \quad (16)$$

In this case, asymptotic solutions of generated power during both short circuit and open circuit become zero. The maximum power, P_{max} , will be obtained at a resistive load corresponding to the impedance matching. Section 3.2.2 obtains an optimized resistive load and the optimized size of PEH skin that generates maximum power.

3.2.2 Impedance Matching for Power Maximization

The maximum output power is obtained from a derivative of the power function expressed previously in Equation (10) (Beeby, Tudor et al. 2006). The mathematical

expression described as:

$$\left. \frac{\partial P}{\partial R_L} \right|_{R_L=R_L^{opt}} = 0 \quad (17)$$

can be reduced to:

$$R_L^{opt} = \frac{h_p}{\omega \bar{\epsilon}_{33}^S A} \quad (18)$$

By substituting Equation (18) into Equation (10), the maximum power output can be derived as:

$$P_{\max} = \frac{\omega \bar{\epsilon}_{31}^2 h_p A (\widetilde{S}_1 + \widetilde{S}_2)^2}{2 \bar{\epsilon}_{33}^S} \quad (19)$$

To solve for the maximum power expressed in Equation (19), four terms must be determined: thickness of PZT, h_p , target system frequency, ω , permittivity at constant strain, $\bar{\epsilon}_{33}^S$ and PEH skin size, A . Of these four terms, the values of h_p and $\bar{\epsilon}_{33}^S$ are already known, since they are known for the piezoelectric material chosen: PSI-5H4E (Piezo Systems, Inc.). In addition, the target system frequency, ω , is also a known variable once the target system is selected.

If we change the position of the remaining variables, Equation (18) can be written

as:

$$A = \frac{h_p}{\omega^{target} \bar{\epsilon}_{33}^S R_L^{target}} \quad (20)$$

We also know the exact value of the external resistive load once the target application is determined. As such, the four variables found in Equation (20) are all known variables. As a result, the PEH skin size that satisfies the maximum output power can be determined by solving Equation (20).

Chapter 4. Experimental Validation

Chapter 4 presents experimental validations of the analytical analysis of the PEH skin presented in section 3. Section 4.1 introduces the test bed for the experiment. Section 4.2 shows the experimental results that demonstrate the validity of the idea proposed in section 3.2.

4.1 Experimental Setup

Figure 4-1 shows the experimental setup: (a) a laptop computer for data processing; (b) an acceleration data acquisition system; (c) a function generator; (d) a fixed gain amplifier; (e) a voltage data acquisition system; (f) an electrical resistive load; (g) a PEH skin with a clamping device; and (h) an electromagnetic shaker.

The PEH skin was fully clamped onto an electromagnetic shaker (Model ET-132-2, Labworks Inc.). To get acceleration data, a small accelerometer was attached close to the center of the PEH skin, as shown in Figure 4-2.

Target system frequency was assumed to be the fundamental mode frequency of the PEH skin, which was simulated using ANSYS software (69.5 Hz). The size of the substrate was 25×25 cm and the sizes of the PZT ranged from 3 cm to 7 cm.

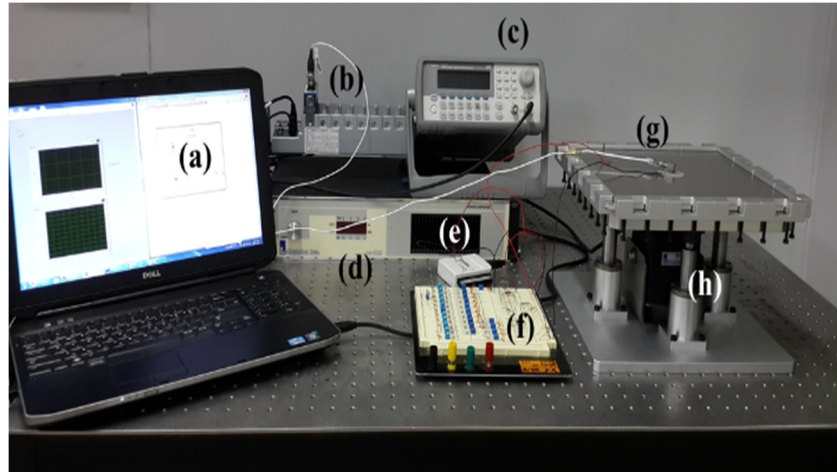


Figure 4-1 Experimental setup

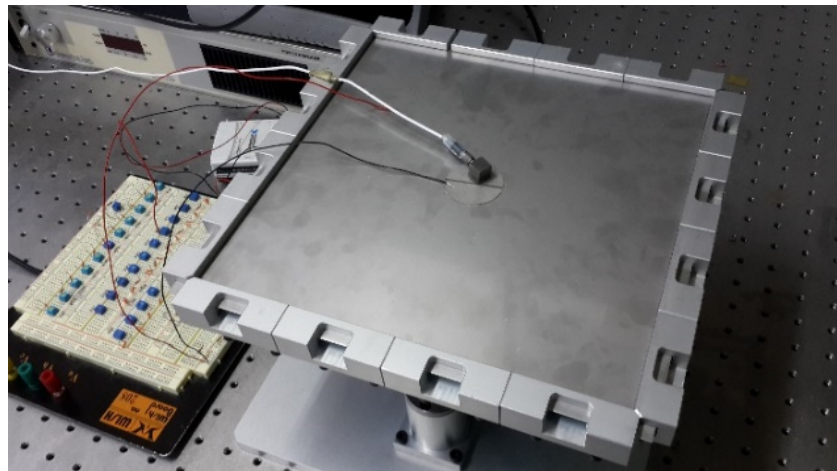
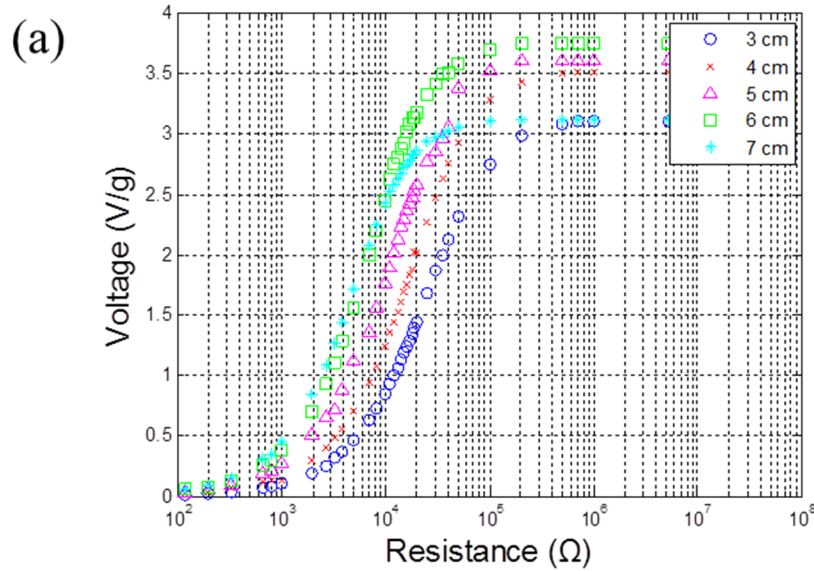


Figure 4-2 Close view of the PEH skin with a clamping device

4.2 Experimental Results

4.2.1 Validation of Limiting Behavior

Figure 4-3 shows the experimental results of asymptotic analysis of the PEH skin studied in the previous sections. According to Figure 4-3 (a), the output voltage generated increases as resistance increases. The slope of the curve is proportional to the size of the PEH skin. However, the opposite is true of the output current, as shown Figure 4-3 (b). Output current decreases as resistance increases. The maximum output power from the PEH skin is achieved at a specific external load, as shown in Figure 4-3 (c). The optimized resistive load in the bigger PEH skin is larger than that of in the smaller PEH skin. Figure 4-3 shows that the experimental results are consistent with the limiting behavior predicted using the analytical model proposed in section 3.2.1.



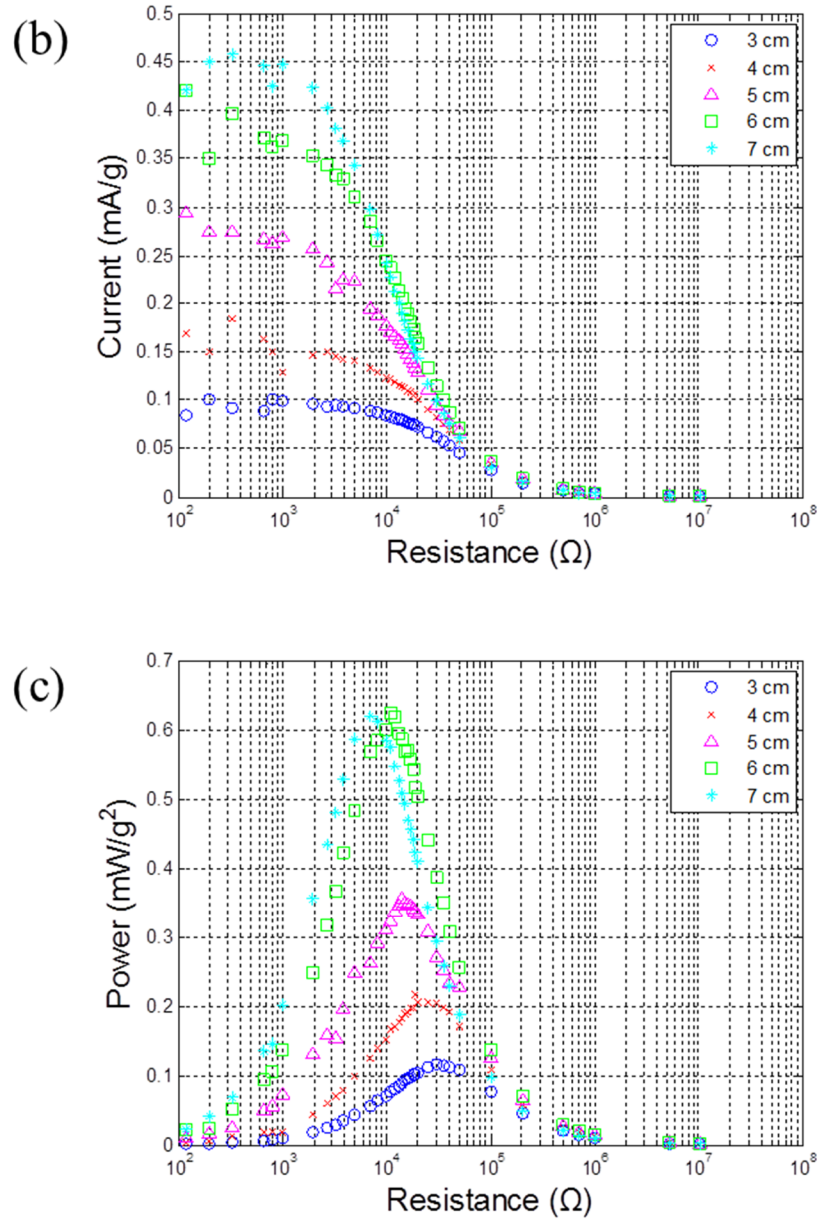
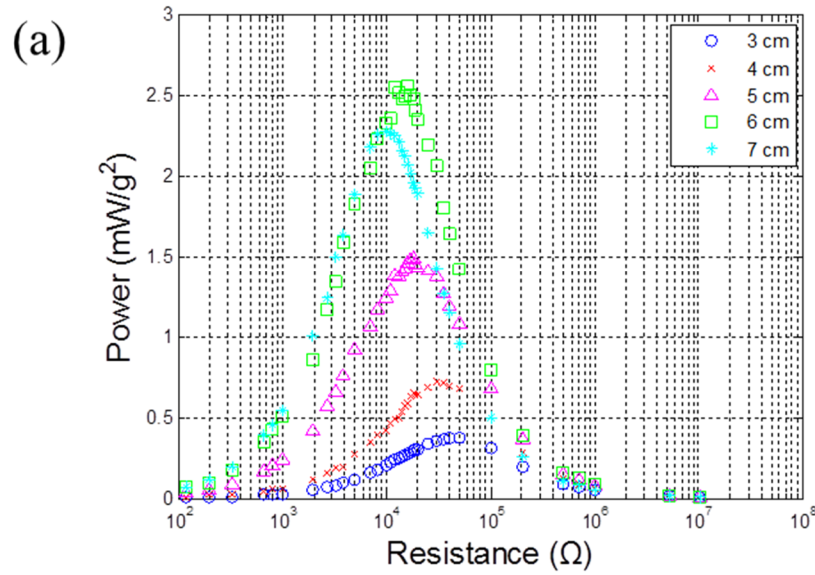


Figure 4-3 Limiting behavior validation for harvested (a) voltage, (b) current, and (c) power

4.2.2 Validation of Optimized PEH Skin Size

Generally, the impedance matching process requires adjusting the load impedance to match the source impedance. However, section 3.2.2 proposes a new way of impedance matching for use during PEH skin design. This new method uses electromechanical characteristics of the chosen piezoelectric material. This section shows the validity of the suggested idea by comparing its predictions with experimental results.

Figure 4-4 shows the output power at different frequencies.



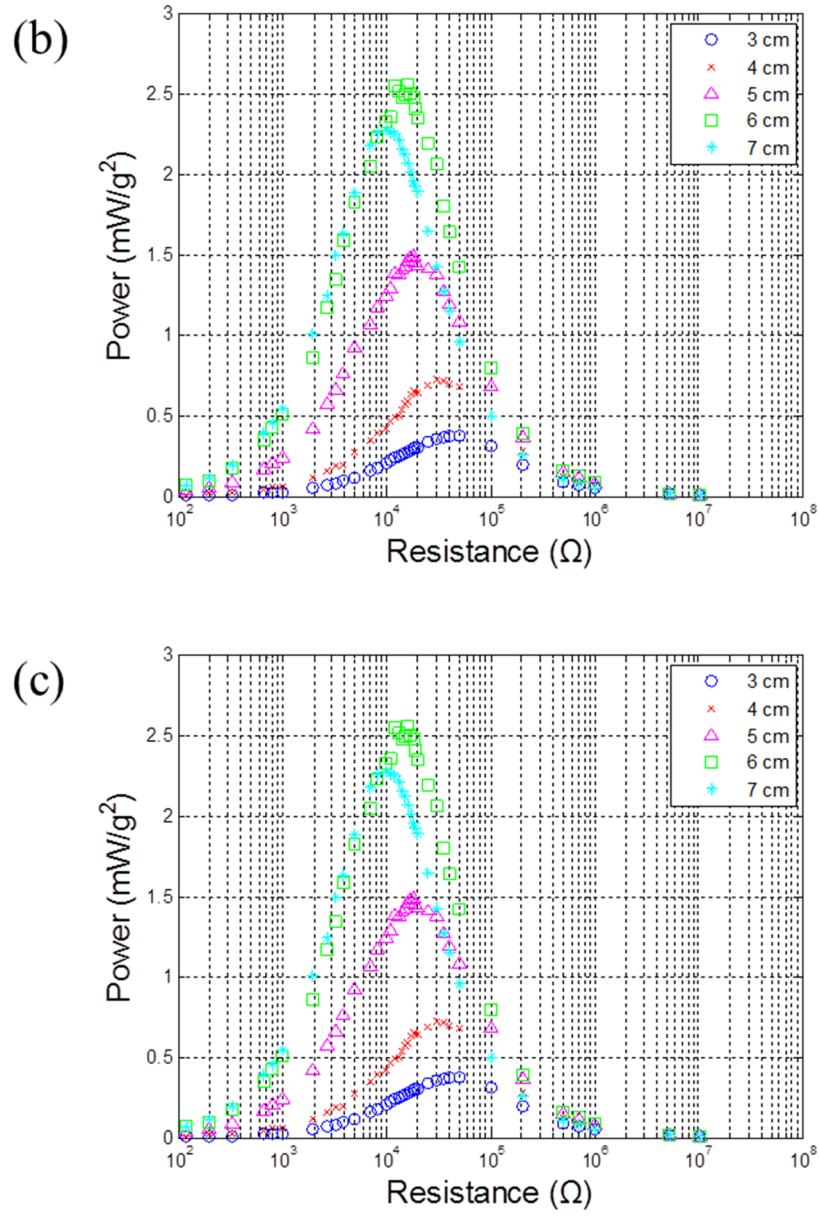


Figure 4-4 Comparison of the output power at (a) 48.65 Hz, (b) 69.5 Hz, and (c) 90.35 Hz

Table 2 Summary of optimum load derived from both the mathematical model and the experiments (Unit: Ω)

Diameter (cm)	48.65 Hz		69.5 Hz		90.35 Hz	
	Model	Exp.	Model	Exp.	Model	Exp.
3	48.3k	50.1 k	33.8 k	30.1k	26.0k	25.0 k
4	27.2 k	30.1 k	19.0 k	19.0k	14.6k	14.0 k
5	17.4 k	17.9 k	12.2 k	13.2k	9.3 k	10.0 k
6	12.1 k	12.1 k	8.5 k	10.0k	6.5 k	7.0 k
7	8.9 k	9.0 k	6.2 k	6.5k	4.8 k	5.0 k

The optimum loads derived from both Equation (18) and the experimental results are shown in Figure 4-4 are arranged in Table 2.

The objective of this study was to verify the accuracy of the PEH skin size derived from Equation (20). To demonstrate this experimentally, the optimal loads obtained in Table 2 were set as the target system loads. Next, the sizes of each PEH skin were calculated using Equation (20). Table 3 presents a summary of the calculated results.

The average difference between the actual size and the calculated size of the PEH skin was approximately 2.8%. The maximum difference was 8% at the 6 cm diameter in the 69.5 Hz case; however, this result seems to be caused by experiment error because it is the lone outlier in the experiment.

As shown in Table 3, if we know the resistive impedance of the target application and the target system frequency, the optimal PEH skin size can be determined during the design process.

Table 3 Backward estimation of the PEH skin size

Diameter (cm)	48.65 Hz		69.5 Hz		90.35 Hz	
	Load (Ω)	D. (cm)	Load (Ω)	D. (cm)	Load (Ω)	D. (cm)
3	50.1 k	2.95	30.1 k	3.18	25.0k	3.06
4	30.1 k	3.80	19.0 k	4.00	14.0k	4.09
5	17.9 k	4.93	13.2 k	4.80	10.0 k	4.84
6	12.1 k	5.99	10.0 k	5.52	7.0 k	5.78
7	9.0 k	6.95	6.5 k	6.84	5.0 k	6.84

Chapter 5. Conclusion

5.1 Contributions

Impedance matching is generally achieved by adjusting resistive load. However, this study proposed a new way of impedance matching for power usage maximization in piezoelectric energy harvesting for specific target. The newly proposed method was enabled by focusing on the electromechanical interaction between the mechanical and the electrical state in piezoelectric material.

The proposed new impedance matching method for power usage maximization during the design process offers several contributions to the field.

First, the suggested method can be used to maximize the power usage for a specific target application from the PEH skin. The level of harvested power from the PEH skin is roughly $\mu\text{W}\sim\text{mW}$. To operate in the target application (like wireless sensors) without problems, the power harvested from the PEH skin should be transferred to the target applications as completely and efficiently as possible because the amount of generated power is small. The proposed design does not need dummy impedance because source impedance is adjusted by the size of the PEH skin. As a result, using this new method, power output in the target application can be maximized in the proposed design due to a nonexistence of dummy impedance.

Second, the proposed idea enables mass production of PEH skin for commercial

use because it enables the PEH skin to be combined with a wireless sensor. In this case, the product only has to consider the system frequency of the target application or surrounding environment.

Finally, the proposed design offers economic advantages. The material cost of the PZT is expensive. Using the new method to decide the exact size of the PEH skin that provides the required power for operating the target application can save expensive material costs during manufacturing.

5.2 Future Work

This thesis identifies two areas of future work that can further develop the idea proposed here.

First, this study considers only the resistive load in impedance matching. However, impedance of commercial products (such as wireless sensors) is composed of resistor, conductor, and inductor. Thus, considering other electronic components will help to further optimize the method for use in practical applications.

Second, in the work outlined in this thesis, the experimental validations were conducted in well-controlled conditions. Input force was harmonic vibration and the boundary condition of the PEH skin was a fully clamped condition. However, real-world operating environments of a PEH skin are dissimilar to the well-controlled conditions in the laboratory. Therefore, demonstration of the proposed method in a

commercial product (like an outdoor air-conditioning unit) will help ascertain the validity of using this technique to optimize PEH skin for practical uses.

Bibliography

Standards Committee of the IEEE Ultrasonics, Ferroelectrics, and Frequency Control Society.

(1988). "IEEE Standard on Piezoelectricity." ANSI/IEEE Std 176-1987: 0_1.

Badel, A., et al. (2006). "Piezoelectric energy harvesting using a synchronized switch technique." Journal of Intelligent Material Systems and Structures **17**(8-9): 831-839.

Beeby, S. P., et al. (2006). "Energy harvesting vibration sources for microsystems applications." Measurement science and technology **17**(12): R175.

Cook-Chennault, K., et al. (2008). "Powering MEMS portable devices—a review of non-regenerative and regenerative power supply systems with special emphasis on piezoelectric energy harvesting systems." Smart Materials and Structures **17**(4): 043001.

Curie, J. and P. Curie (1880). "Développement, par pression, de l'électricité polaire dans les cristaux hémiedres à faces inclinées." Comptes Rendus **91**: 291-295.

DuToit, N. E. and B. L. Wardle (2007). "Experimental verification of models for microfabricated piezoelectric vibration energy harvesters." AIAA journal **45**(5): 1126-1137.

Dutoit, N. E., et al. (2005). "Design considerations for MEMS-scale piezoelectric mechanical vibration energy harvesters." Integrated Ferroelectrics **71**(1): 121-160.

Erturk, A. (2011). "Piezoelectric energy harvesting for civil infrastructure system applications:

Moving loads and surface strain fluctuations." Journal of Intelligent Material Systems and Structures **22**(17): 1959-1973.

Erturk, A. and D. Inman (2009). "An experimentally validated bimorph cantilever model for piezoelectric energy harvesting from base excitations." Smart Materials and Structures **18**(2): 025009.

Erturk, A. and D. J. Inman (2008). "On mechanical modeling of cantilevered piezoelectric vibration energy harvesters." Journal of Intelligent Material Systems and Structures **19**(11): 1311-1325.

Erturk, A., et al. (2009). "Effect of strain nodes and electrode configuration on piezoelectric energy harvesting from cantilevered beams." Journal of vibration and acoustics **131**(1).

Gautschi, G. (2002). Piezoelectric sensorics: force, strain, pressure, acceleration and acoustic emission sensors, materials and amplifiers, Springer.

Higashihata, Y., et al. (1986). "Piezoelectric properties and applications in the composite system of vinylidene fluoride and trifluoroethylene copolymer and PZT ceramics." Ferroelectrics **68**(1): 63-75.

Kim, H., et al. (2007). "Consideration of impedance matching techniques for efficient piezoelectric energy harvesting." Ultrasonics, Ferroelectrics and Frequency Control, IEEE Transactions on **54**(9): 1851-1859.

Kong, N., et al. (2010). "Resistive impedance matching circuit for piezoelectric energy harvesting." Journal of Intelligent Material Systems and Structures **21**(13): 1293-1302.

Lee, S. and B. D. Youn (2011). "A new piezoelectric energy harvesting design concept: multimodal energy harvesting skin." Ultrasonics, Ferroelectrics and Frequency Control, IEEE Transactions on **58**(3): 629-645.

Lee, S., et al. (2009). "Robust segment-type energy harvester and its application to a wireless sensor." Smart Materials and Structures **18**(9): 095021.

Liang, J. and W.-H. Liao (2011). "Energy flow in piezoelectric energy harvesting systems." Smart Materials and Structures **20**(1): 015005.

Manbachi, A. and R. S. Cobbold (2011). "Development and application of piezoelectric materials for ultrasound generation and detection." Ultrasound **19**(4): 187-196.

Rao, S. S. (2003). "Mechanical Vibrations, 4/E", Pearson Education India.

Skoog, D. A., et al. (1998). "Principles of instrumental analysis, 6/E", Cengage Learning

Sodano, H. A., et al. (2004). "A review of power harvesting from vibration using piezoelectric materials." Shock and Vibration Digest **36**(3): 197-206.

Stephen, N. (2006). "On energy harvesting from ambient vibration." Journal of Sound and Vibration **293**(1): 409-425.

Vinogradov, A. M., et al. (2004). "Damping and electromechanical energy losses in the piezoelectric polymer PVDF." Mechanics of Materials **36**(10): 1007-1016.

국문 초록

요즘, 우리 주변에서 버려지고 있는 미세한 진동 에너지로부터 전기 에너지를 수확하는 압전 에너지 하베스팅 기술이 무선 센서 등 소형 전자기기의 배터리를 대체하는 해결책으로 급부상하고 있다. 이전의 압전 에너지 하베스팅 장치 연구는 공진 현상을 이용하여 큰 변형률로부터 많은 양의 전기 에너지를 수확하기 위하여 외팔보 형태의 장치 연구에 집중되어 왔다. 이러한 장점에도 불구하고, 외팔보 형태의 압전 에너지 하베스팅 장치는 세가지 단점 때문에 실용성에 한계가 있었다. 첫째, 외팔보 형태의 압전 에너지 하베스팅 장치는 무게 추와 고정 장치의 존재로 인하여 많은 공간을 필요로 한다. 둘째, 외팔보 형태의 압전 에너지 하베스팅 장치는 외부 충격과 오염 물질에 취약하다. 마지막으로, 외팔보 형태의 압전 에너지 하베스팅 장치를 장기간 사용할 경우 고정 장치가 느슨해지며 전력 수확량이 줄어들게 된다. 이러한 단점들을 극복하기 위하여, 진동 구조체 표면에 얇은 압전 박막을 직접 붙여 전기 에너지를 수확하는 압전 에너지 하베스팅 스킨이 외팔보 형태의 압전 에너지 하베스팅 장치의 대안으로 떠올랐다. 지금까지 압전 에너지 하베스팅 스킨 연구는 전압 상쇄 효과를 최소화 시키기 위하여 변형률 변곡선의 설계에 집중하였다.

본 연구에서는 외부 부하의 크기에 맞춰 가용 전력을 극대화시킬 수 있도록 압전 에너지 하베스팅 스킨의 임피던스 매칭 변수 최적화를 새롭게 제안하였다. 제안된 설계 과정은 다음의 세 단계로 구성된다. 첫 번째, 압전 에너지 하베스팅 스킨의 출력 전력량이 측정 가능한 변수들로 표현하였다. 두 번째, 압전 에너지 하베스팅 스킨의 점근 분석을 통해 압전

에너지 하베스팅 스킨의 특성을 알아내었다. 마지막으로, 특정 외부 부하의 크기에 맞춰 가용 전력을 극대화 시킬 수 있는 압전 에너지 하베스팅 스킨의 최적화된 크기를 밝혔다. 본 연구에서 제안된 방법의 유효성은 실험을 통해 입증하였으며, 이론적 분석과 실험적 결과가 잘 일치함을 확인할 수 있었다.

주요어: 압전

에너지 하베스팅

압전 에너지 하베스팅 스킨

임피던스 매칭

학 번: 2012-20707

본 연구는 2013년도 BK 21 플러스 사업에 의하여 지원되었으며,
이에 감사 드립니다.